

Articles

Reactions of Doubly Bridged Biscyclopentadienes with Molybdenum (Tungsten) Carbonyl

Baiquan Wang,* Bolin Zhu, Shansheng Xu, and Xiuzhong Zhou

Department of Chemistry, State Key Laboratory of Elemento-Organic Chemistry, Nankai University, Tianjin 300071, People's Republic of China

Received July 15, 2003

Dimolybdenum complexes (X)(Y)[(η^5 -C₅H₃)Mo(CO)₃]₂ [Y = Me₂Si, X = Me₂C, (CH₂)₅C, CH₂; Y = Ph₂Si, X = Me₂C] and desilylation products (X)[(η^5 -C₅H₄)Mo(CO)₃]₂ were obtained from the reactions of carbon and silicon doubly bridged biscyclopentadiene ligands (X)(Y)(C₅H₄)₂ with Mo(CO)₆ in refluxing xylene. When these ligands reacted with W(CO)₆, under similar conditions, in addition to ditungsten complexes (X)(Y)[(η^5 -C₅H₃)W(CO)₃]₂ [X = Me₂C; Y = Me₂Si, Ph₂Si] and desilylation products (X)[(η^5 -C₅H₄)W(CO)₃]₂, a class of structurally novel complexes (X)(η^5 -C₅H₃)(η^5 , η^1 -C₅H₃)(Y)W(CO)₃[W(CO)₃] [for X = Me₂C, (CH₂)₅C; Y = Me₂-Si] with a W–Si bond were also isolated. The reactions of carbon and germanium doubly bridged biscyclopentadiene ligands (X)(Me₂Ge)(C₅H₄)₂ [X = Me₂C, (CH₂)₅C] with Mo(CO)₆ or W(CO)₆ gave similar novel complexes (X)(η^5 -C₅H₃)(η^5 , η^1 -C₅H₃)(Me₂Ge)M(CO)₃[M(CO)₃] [X = Me₂C, (CH₂)₅C; M = Mo, W] with a M–Ge bond. The reactions also produced degermylation products. However, the corresponding dimolybdenum or ditungsten complexes were not isolated in these cases. The molecular structures of **2**, **6**, **8**, **10**, **11**, **13**, **14**, **15**, **19**, **21**, **22**, **25t**, and **26t** have been determined by X-ray diffraction. The M–M distances in complexes **2** [3.4328(12) Å], **8** [3.453(2) Å], and **11** [3.403(2) Å] are conspicuously elongated and are in fact the longest ever reported among the biscyclopentadienyl dimolybdenum or ditungsten complexes. The factors affecting the structures of dimolybdenum or ditungsten complexes are discussed.

Introduction

Considerable attention has been focused on the synthesis and chemical behavior of a variety of doubly bridged biscyclopentadienyl carbonyl dimetallic complexes (M = Ti, V, Cr, Fe, Ru, Co, Ni).¹ Compared to their nonbridged and single-bridged analogues, these complexes exhibit unique characteristics in both their structures and reactivity. Reactions of doubly bridged biscyclopentadiene (C₅H₄)₂(SiMe₂)₂ with metal carbonyl compounds have been extensively studied in the past decade.^{2,3} We have recently investigated the reaction of a certain type of doubly bridged biscyclopentadiene ligands with Fe(CO)₅ and obtained a series of diiron

complexes with superlong Fe–Fe bond distances and novel complexes with Fe–Si or Fe–Ge bonds.⁴ This paper will further report the reaction of the doubly bridged biscyclopentadiene ligands with molybdenum and tungsten carbonyl.

Experimental Section

General Considerations. Schlenk and vacuum line techniques were employed for all manipulations. All solvents were distilled from appropriate drying agents under argon prior to use. ¹H NMR spectra were recorded on a Bruker AC-P200, while IR spectra were recorded as KBr disks on a Nicolet 560 E.S.P. FTIR spectrometer. Mass spectra were obtained from a VG ZAB-HS. EPR spectra were recorded on a Bruker EMX instrument. Elemental analyses were performed on a Perkin-

* Corresponding author. Fax: 86-22-23502458. E-mail: bqwang@nankai.edu.cn.

(1) Corey, J. Y.; Huhmann, J. L.; Rath, N. P. *Inorg. Chem.* **1995**, *34*, 3203, and references therein.

(2) (a) Amor, F.; Gomez-Sal, P.; Jesus, E.; Royo, P.; Vazquez de Miguel, A. *Organometallics* **1994**, *13*, 4322. (b) Amor, F.; Jesus, E.; Perez, A. I.; Royo, P.; Vazquez de Miguel, A. *Organometallics* **1996**, *15*, 365. (c) Amor, F.; Gomez-Sal, P.; Jesus, E.; Martin, A.; Perez, A. I.; Royo, P.; Vazquez de Miguel, A. *Organometallics* **1996**, *15*, 2103. (d) Galakhov, M. V.; Gil, A.; Jesus, E.; Royo, P. *Organometallics* **1995**, *14*, 3746. (e) Calvo, M.; Galakhov, M. V.; Gomez-Garcia, R.; Gomez-Sal, P.; Martin, A.; Royo, P.; Vazquez de Miguel, A. *J. Organomet. Chem.* **1997**, *548*, 157. (f) Amor, F.; de Justes, F.; Royo, P.; de Miguel, A. V. *Inorg. Chem.* **1996**, *35*, 3440. (g) Calvo, M.; Gomez-Sal, P.; Manzanero, A.; Royo, P. *Polyhedron* **1998**, *17*, 1081. (h) Gomez-Gacia, R.; Royo, P. *J. Organomet. Chem.* **1999**, *583*, 86.

(3) (a) McKinley S. G.; Angelici, R. J. *Organometallics* **2002**, *21*, 1235. (b) Ovchinnikov, M. V.; Angelici, R. J. *J. Am. Chem. Soc.* **2000**, *122*, 6130. (c) Ovchinnikov, M. V.; Guzei, I. A.; Angelici, R. J. *Organometallics* **2001**, *20*, 691. (d) Ovchinnikov, M. V.; Wang, X.; Schultz, A. J.; Guzei, I. A.; Angelici, R. J. *Organometallics* **2002**, *21*, 3292. (e) Ovchinnikov, M. V.; Ellern, A. M.; Guzei, I. A.; Angelici, R. J. *Inorg. Chem.* **2001**, *40*, 7014. (f) Ovchinnikov, M. V.; LeBlanc, E.; Guzei, I. A.; Angelici, R. J. *J. Am. Chem. Soc.* **2001**, *123*, 11494. (g) Ovchinnikov, M. V.; Klein, D. P.; Guzei, I. A.; Choi, M. G.; Angelici, R. J. *Organometallics* **2002**, *21*, 617.

(4) (a) Xu, S.; Zhang, J.; Zhu, B.; Wang, B.; Zhou, X.; Weng, L. *J. Organomet. Chem.* **2001**, *626*, 186. (b) Wang, B.; Zhu, B.; Zhang, J.; Xu, S.; Zhou, X.; Weng, L. *Organometallics* **2003**, submitted.

Elmer 240C analyzer. $(\text{Me}_2\text{C})(\text{Me}_2\text{Si})(\text{C}_5\text{H}_4)_2$ (**1**),⁵ $[\text{CH}_2]_5\text{C}(\text{Me}_2\text{Si})(\text{C}_5\text{H}_4)_2$ (**4**),⁴ $(\text{Me}_2\text{C})(\text{Ph}_2\text{Si})(\text{C}_5\text{H}_4)_2$ (**7**),⁴ $(\text{CH}_2)(\text{Me}_2\text{Si})(\text{C}_5\text{H}_4)_2$ (**9**),⁴ $(\text{Me}_2\text{C})(\text{Me}_2\text{Ge})(\text{C}_5\text{H}_4)_2$ (**18**),⁵ $[\text{CH}_2]_5\text{C}(\text{Me}_2\text{Ge})(\text{C}_5\text{H}_4)_2$ (**20**),⁴ and $(\text{Me}_2\text{C})(\text{Me}_2\text{Si})(t\text{-BuC}_5\text{H}_3)_2$ (**24**)⁴ were prepared according to literature methods.

Reaction of $(\text{Me}_2\text{C})(\text{Me}_2\text{Si})(\text{C}_5\text{H}_4)_2$ (1**) with $\text{Mo}(\text{CO})_6$.** A solution of 0.40 g (1.75 mmol) of $(\text{Me}_2\text{C})(\text{Me}_2\text{Si})(\text{C}_5\text{H}_4)_2$ (**1**) and 0.80 g (3.03 mmol) of $\text{Mo}(\text{CO})_6$ in 40 mL of xylene was refluxed for 6.5 h. After removal of solvent the residue was chromatographed on an alumina column using petroleum ether/ CH_2Cl_2 as eluent. The first band (red) afforded 0.03 g (3%) of **3** as deep red crystals. The second band (green) gave 0.19 g (18%) of **2** as black crystals. **2**: mp 220 °C (dec). Anal. Calcd for $\text{C}_{21}\text{H}_{18}\text{Mo}_2\text{O}_6\text{Si}$: C, 43.02; H, 3.09. Found: C, 42.67; H, 3.18. ¹H NMR (CDCl_3) δ : 5.36 (m, 2H, C_5H_3), 5.21 (m, 2H, C_5H_3), 5.07 (m, 2H, C_5H_3), 1.50 (s, 3H, C-Me), 1.35 (s, 3H, C-Me), 0.55 (s, 3H, Si-Me), 0.46 (s, 3H, Si-Me). IR (ν_{CO} , cm^{-1}): 2026(s), 1938(s), 1920(s), 1896(s), 1870(s). MS (EI): m/z 586 (M^+ , 8.5), 558 ($\text{M}^+ - \text{CO}$, 22.5), 530 ($\text{M}^+ - 2\text{CO}$, 8.9), 502 ($\text{M}^+ - 3\text{CO}$, 38.7), 474 ($\text{M}^+ - 4\text{CO}$, 84.6), 472 ($\text{M}^+ - 2\text{CO} - \text{SiMe}_2$, 90.6), 446 ($\text{M}^+ - 5\text{CO}$, 63.4), 444 ($\text{M}^+ - 3\text{CO} - \text{SiMe}_2$, 70.5), 418 ($\text{M}^+ - 6\text{CO}$, 52.3), 412 (100), 317 ($\text{M}^+ - 6\text{CO} - \text{Mo}$, 6.4), 224 ($\text{M}^+ - 6\text{CO} - 2\text{Mo}$, 16.2). **3**:⁶ mp 200 °C (dec). ¹H NMR (CDCl_3) δ : 5.34 (m, 4H, C_5H_4), 5.22 (m, 4H, C_5H_4), 1.51 (s, 6H, C-Me). IR (ν_{CO} , cm^{-1}): 2002(s), 1960(s), 1946(s), 1914(s), 1894(s), 1878(s), 1864(s).

Reaction of $[(\text{CH}_2)_5\text{C}](\text{Me}_2\text{Si})(\text{C}_5\text{H}_4)_2$ (4**) with $\text{Mo}(\text{CO})_6$.** A solution of 0.30 g (1.12 mmol) of **4** and 0.70 g (2.65 mmol) of $\text{Mo}(\text{CO})_6$ in 40 mL of xylene was refluxed for 6.5 h. After removal of solvent the residue was chromatographed on an alumina column using petroleum ether/ CH_2Cl_2 as eluent. The first band (red) afforded 0.05 g (9%) of **6** as deep red crystals. The second band (green) gave 0.10 g (15%) of **5** as black crystals. **5**: mp 190 °C (dec). Anal. Calcd for $\text{C}_{24}\text{H}_{22}\text{Mo}_2\text{O}_6\text{Si}$: C, 46.02; H, 3.54. Found: C, 45.92; H, 4.18. ¹H NMR (CDCl_3) δ : 5.36 (m, 2H, C_5H_3), 5.20 (m, 4H, C_5H_3), 1.90–1.20 (m, 10H, CH_2), 0.53 (s, 3H, Si-Me), 0.45 (s, 3H, Si-Me). IR (ν_{CO} , cm^{-1}): 2010(s), 1954(s), 1906(s), 1863(m). **6**: mp 230 °C (dec). Anal. Calcd for $\text{C}_{22}\text{H}_{18}\text{Mo}_2\text{O}_6$: C, 46.34; H, 3.18. Found: C, 46.28; H, 3.17. ¹H NMR (CDCl_3) δ : 5.25 (m, 8H, C_5H_4), 1.90–1.35 (m, 10H, CH_2). IR (ν_{CO} , cm^{-1}): 2010(s), 1950(s), 1918(s), 1894(s), 1878(s), 1863(s).

Reaction of $(\text{Me}_2\text{C})(\text{Ph}_2\text{Si})(\text{C}_5\text{H}_4)_2$ (7**) with $\text{Mo}(\text{CO})_6$.** A solution of 0.50 g (1.42 mmol) of **7** and 0.70 g (2.65 mmol) of $\text{Mo}(\text{CO})_6$ in 40 mL of xylene was refluxed for 6.5 h. After removal of solvent the residue was chromatographed on an alumina column using petroleum ether/ CH_2Cl_2 as eluent. The first band (red) gave 0.05 g (7%) of **3**. The second band (green) afforded 0.08 g (8%) of **8** as black crystals. **8**: mp 200 °C (dec). Anal. Calcd for $\text{C}_{31}\text{H}_{22}\text{Mo}_2\text{O}_6\text{Si}$: C, 52.41; H, 3.12. Found: C, 52.36; H, 3.10. ¹H NMR (CDCl_3) δ : 7.60–7.30 (m, 10H, C_6H_5), 5.60 (m, 2H, C_5H_3), 5.50 (m, 2H, C_5H_3), 5.15 (m, 2H, C_5H_3), 1.35 (s, 3H, C-Me), 1.13 (s, 3H, C-Me). IR (ν_{CO} , cm^{-1}): 2015(s), 1956(s), 1945(s), 1890(m), 1874(m).

Reaction of $(\text{H}_2\text{C})(\text{Me}_2\text{Si})(\text{C}_5\text{H}_4)_2$ (9**) with $\text{Mo}(\text{CO})_6$.** A solution of 0.40 g (2.00 mmol) of **9** and 0.70 g (2.65 mmol) of $\text{Mo}(\text{CO})_6$ in 40 mL of xylene was refluxed for 6.5 h. After removal of solvent the residue was chromatographed on an alumina column using petroleum ether/ CH_2Cl_2 as eluent. The red band afforded 0.10 g (9%) of **10** as dark red crystals. **10**: mp 210 °C. Anal. Calcd for $\text{C}_{19}\text{H}_{14}\text{Mo}_2\text{O}_6\text{Si}$: C, 40.88; H, 2.63. Found: C, 40.40; H, 2.39. ¹H NMR (CDCl_3) δ : 5.32 (m, 2H, C_5H_3), 5.27 (m, 4H, C_5H_3), 3.92 (d, $J = 16.0$ Hz, 1H, CH_2), 3.24 (d, $J = 16.0$ Hz, 1H, CH_2), 0.57 (s, 3H, Si-Me), 0.33 (s, 3H, Si-Me). IR (ν_{CO} , cm^{-1}): 2010(s), 1958(s), 1934(m), 1918(m), 1890(s), 1866(s).

Reaction of $(\text{Me}_2\text{C})(\text{Me}_2\text{Si})(\text{C}_5\text{H}_4)_2$ (1**) with $\text{W}(\text{CO})_6$.** A solution of 0.40 g (1.75 mmol) of $(\text{Me}_2\text{C})(\text{Me}_2\text{Si})(\text{C}_5\text{H}_4)_2$ (**1**) and 1.00 g (2.84 mmol) of $\text{W}(\text{CO})_6$ in 40 mL of xylene was refluxed for 24 h. After removal of solvent the residue was chromatographed on an alumina column using petroleum ether/ CH_2Cl_2 as eluent. The first band (yellow) afforded 0.08 g (6%) of **13** as orange crystals. The second band (red) gave 0.05 g (4%) of **12** as deep red crystals. The third band (gray) gave 0.03 g (2%) of **11** as black crystals. **11**: mp 210 °C (dec). Anal. Calcd for $\text{C}_{21}\text{H}_{18}\text{O}_6\text{SiW}_2$: C, 33.09; H, 2.38. Found: C, 33.05; H, 2.46. ¹H NMR (CDCl_3) δ : 5.31 (m, 2H, C_5H_3), 5.27 (m, 4H, C_5H_3), 1.54 (s, 3H, C-Me), 1.36 (s, 3H, C-Me), 0.56 (s, 3H, Si-Me), 0.49 (s, 3H, Si-Me). IR (ν_{CO} , cm^{-1}): 2015(s), 1937(s), 1910(s), 1887(s). **12**:⁶ mp 281–282 °C. ¹H NMR (CDCl_3) δ : 5.26 (m, 8H, C_5H_4), 1.55 (s, 6H, C-Me). IR (ν_{CO} , cm^{-1}): 1997(s), 1958(s), 1910(s), 1885(s), 1870(s), 1858(s). **13**: mp 260 °C (dec). Anal. Calcd for $\text{C}_{21}\text{H}_{18}\text{O}_6\text{SiW}_2$: C, 33.09; H, 2.38. Found: C, 33.24; H, 2.42. ¹H NMR (CDCl_3) δ : 6.20 (m, 1H, C_5H_3), 5.84 (m, 1H, C_5H_3), 5.30 (m, 1H, C_5H_3), 5.19 (m, 1H, C_5H_3), 5.10 (m, 1H, C_5H_3), 4.96 (m, 1H, C_5H_3), 1.60 (s, 3H, C-Me), 1.58 (s, 3H, C-Me), 0.74 (s, 3H, Si-Me), 0.73 (s, 3H, Si-Me). IR (ν_{CO} , cm^{-1}): 2026(s), 1989(s), 1940(s), 1914(s), 1890(s).

Reaction of $[(\text{CH}_2)_5\text{C}](\text{Me}_2\text{Si})(\text{C}_5\text{H}_4)_2$ (4**) with $\text{W}(\text{CO})_6$.** A solution of 1.00 g (3.72 mmol) of **4** and 1.50 g (4.26 mmol) of $\text{W}(\text{CO})_6$ in 40 mL of xylene was refluxed for 24 h. After removal of the solvent the residue was chromatographed on an alumina column using petroleum ether/ CH_2Cl_2 as eluent. The first band (orange) afforded 0.08 g (3%) of **15** as orange crystals. The second band (red) gave 0.03 g (1%) of **14** as dark red crystals. **14**: mp 222 °C (dec). Anal. Calcd for $\text{C}_{22}\text{H}_{18}\text{O}_6\text{W}_2$: C, 35.42; H, 2.43. Found: C, 35.41; H, 2.44. ¹H NMR (CDCl_3) δ : 5.65 (m, 2H, C_5H_4), 5.43 (m, 2H, C_5H_4), 5.16 (m, 2H, C_5H_4), 5.09 (m, 2H, C_5H_4), 1.90–1.20 (m, 10H, CH_2). IR (ν_{CO} , cm^{-1}): 2002(s), 1946(s), 1914(s), 1886(s), 1868(s), 1850(s). **15**: mp 260 °C (dec). Anal. Calcd for $\text{C}_{24}\text{H}_{22}\text{O}_6\text{SiW}_2$: C, 35.93; H, 2.76. Found: C, 35.91; H, 2.67. ¹H NMR (CDCl_3) δ : 6.31 (m, 1H, C_5H_3), 5.85 (m, 1H, C_5H_3), 5.27 (m, 2H, C_5H_3), 5.10 (m, 1H, C_5H_3), 4.95 (m, 1H, C_5H_3), 2.10–1.30 (m, 10H, CH_2), 0.71 (s, 6H, Si-Me). IR (ν_{CO} , cm^{-1}): 2026(s), 1989(s), 1954(m), 1910(s), 1880(s).

Reaction of $(\text{Me}_2\text{C})(\text{Ph}_2\text{Si})(\text{C}_5\text{H}_4)_2$ (7**) with $\text{W}(\text{CO})_6$.** A solution of 1.00 g (2.84 mmol) of **7** and 1.50 g (4.26 mmol) of $\text{W}(\text{CO})_6$ in 40 mL of xylene was refluxed for 24 h. After removal of the solvent the residue was chromatographed on an alumina column using petroleum ether/ CH_2Cl_2 as eluent. The first band (red) gave 0.11 g (6%) of **12**. The second band (gray) afforded 0.03 g (1%) of **16** as black crystals. **16**: mp 230 °C (dec). Anal. Calcd for $\text{C}_{31}\text{H}_{22}\text{W}_2\text{O}_6\text{Si}$: C, 42.01; H, 2.50. Found: C, 41.68; H, 2.44. ¹H NMR (CDCl_3) δ : 7.60–7.45 (m, 4H, C_6H_5), 7.40–7.25 (m, 6H, C_6H_5), 5.72 (m, 2H, C_5H_3), 5.40 (m, 2H, C_5H_3), 5.36 (m, 2H, C_5H_3), 1.37 (s, 3H, C-Me), 1.16 (s, 3H, C-Me). IR (ν_{CO} , cm^{-1}): 2010(s), 1962(s), 1946(s), 1922(s), 1898(s), 1859(m).

Reaction of $(\text{H}_2\text{C})(\text{Me}_2\text{Si})(\text{C}_5\text{H}_4)_2$ (9**) with $\text{W}(\text{CO})_6$.** A solution of 0.40 g (2.00 mmol) of **9** and 1.00 g (2.84 mmol) of $\text{W}(\text{CO})_6$ in 40 mL of xylene was refluxed for 24 h. After removal of the solvent the residue was chromatographed on an alumina column using petroleum ether/ CH_2Cl_2 as eluent. The red band afforded 0.18 g (18%) of **17** as dark red crystals. **17**:⁷ mp 220 °C (dec) (lit. 226–228 °C dec⁷). ¹H NMR (CDCl_3) δ : 5.28 (m, 8H, C_5H_4), 3.88 (s, 2H, CH_2). IR (ν_{CO} , cm^{-1}): 1997(s), 1946(s), 1878(s), 1859(s).

Reaction of $(\text{Me}_2\text{C})(\text{Me}_2\text{Ge})(\text{C}_5\text{H}_4)_2$ (18**) with $\text{Mo}(\text{CO})_6$.** A solution of 0.60 g (2.20 mmol) of **18** and 0.80 g (3.03 mmol) of $\text{Mo}(\text{CO})_6$ in 40 mL of xylene was refluxed for 7 h. After removal of solvent the residue was chromatographed on an alumina column using petroleum ether/ CH_2Cl_2 as eluent. The first band (yellow) afforded 0.10 g (7%) of **19** as orange-red

(5) Nifant'ev, I. E.; Yarnykh, V. L.; Borzov, M. V.; Mazurchik, B. A.; Mstyslasky, V. I.; Roznyatovsky, V. A.; Ustyynyuk, Y. A. *Organometallics* **1991**, *10*, 3739.

(6) Fierro, R.; Bitterwolf, T. E.; Rheingold, A. L.; Yap, G. P. A.; Liable-Sands, L. M. *J. Organomet. Chem.* **1996**, *524*, 19.

(7) Bitterwolf, T. E.; Rheingold, A. L. *Organometallics* **1991**, *10*, 3856.

crystals. The second band (red) afforded 0.25 g (22%) of **3**. **19**: mp 250 °C (dec). Anal. Calcd for $C_{21}H_{18}GeMo_2O_6$: C, 39.98; H, 2.88. Found: C, 39.51; H, 2.74. 1H NMR ($CDCl_3$) δ : 5.98 (m, 1H, C_5H_3), 5.69 (m, 1H, C_5H_3), 5.37 (m, 1H, C_5H_3), 5.18 (m, 1H, C_5H_3), 5.00 (m, 1H, C_5H_3), 4.90 (m, 1H, C_5H_3), 1.55 (s, 3H, C-Me), 1.53 (s, 3H, C-Me), 0.82 (s, 6H, Ge-Me). IR (ν_{CO} , cm^{-1}): 2034(s), 1993(s), 1954(s), 1934(s), 1918(s), 1902(s).

Reaction of $[(CH_2)_5C](Me_2Ge)(C_5H_4)_2$ (20**) with $Mo(CO)_6$.** A solution of 0.50 g (1.60 mmol) of **20** and 1.00 g (3.79 mmol) of $Mo(CO)_6$ in 40 mL of xylene was refluxed for 6.5 h. After removal of solvent the residue was chromatographed on an alumina column using petroleum ether/ CH_2Cl_2 as eluent. The first band (red) afforded 0.15 g (16%) of **6**. The second band (green) gave 0.10 g (10%) of **21** as black crystals. **21**: mp 210 °C (dec). Anal. Calcd for $C_{24}H_{22}GeMo_2O_6$: C, 42.97; H, 3.31. Found: C, 42.89; H, 3.32. 1H NMR ($CDCl_3$) δ : 6.08 (m, 1H, C_5H_3), 5.69 (m, 1H, C_5H_3), 5.36 (m, 1H, C_5H_3), 5.27 (m, 1H, C_5H_3), 4.97 (m, 1H, C_5H_3), 4.90 (m, 1H, C_5H_3), 2.10–1.30 (m, 10H, CH_2), 0.81 (s, 3H, Ge-Me), 0.79 (s, 3H, Ge-Me). IR (ν_{CO} , cm^{-1}): 2026(s), 1989(s), 1962(s), 1922(s), 1886(s).

Reaction of $(Me_2C)(Me_2Ge)(C_5H_4)_2$ (18**) with $W(CO)_6$.** A solution of 0.80 g (3.03 mmol) of **18** and 1.50 g (4.26 mmol) of $W(CO)_6$ in 40 mL of xylene was refluxed for 24 h. After removal of the solvent the residue was chromatographed on an alumina column using petroleum ether/ CH_2Cl_2 as eluent. The first band (yellow) afforded 0.08 g (3%) of **22** as orange-red crystals. The second band (red) afforded 0.12 g (6%) of **12**. **22**: mp 285 °C (dec). Anal. Calcd for $C_{21}H_{18}GeO_6W_2$: C, 31.27; H, 2.38. Found: C, 31.20; H, 2.24. 1H NMR ($CDCl_3$) δ : 6.20 (m, 1H, C_5H_3), 5.86 (m, 1H, C_5H_3), 5.25 (m, 1H, C_5H_3), 5.21 (m, 1H, C_5H_3), 5.13 (m, 1H, C_5H_3), 4.94 (m, 1H, C_5H_3), 1.58 (s, 6H, C-Me), 0.82 (s, 6H, Ge-Me). IR (ν_{CO} , cm^{-1}): 2034(s), 1988(s), 1941(s), 1924(s), 1910(s), 1894(s).

Reaction of $[(CH_2)_5C](Me_2Ge)(C_5H_4)_2$ (20**) with $W(CO)_6$.** A solution of 1.00 g (3.20 mmol) of **20** and 1.50 g (4.26 mmol) of $W(CO)_6$ in 40 mL of xylene was refluxed for 24 h. After removal of the solvent the residue was chromatographed on an alumina column using petroleum ether/ CH_2Cl_2 as eluent. The first band (orange) afforded 0.10 g (4%) of **23** as orange crystals. The second band (red) gave 0.03 g (1%) of **14**. **23**: mp 230 °C (dec). Anal. Calcd for $C_{24}H_{22}GeMo_2O_6$: C, 34.04; H, 2.62. Found: C, 34.08; H, 2.66. 1H NMR ($CDCl_3$) δ : 6.29 (m, 1H, C_5H_3), 5.85 (m, 1H, C_5H_3), 5.28 (m, 1H, C_5H_3), 5.23 (m, 1H, C_5H_3), 5.13 (m, 1H, C_5H_3), 4.94 (m, 1H, C_5H_3), 2.10–1.20 (m, 10H, CH_2), 0.81 (s, 3H, Ge-Me), 0.78 (s, 3H, Ge-Me). IR (ν_{CO} , cm^{-1}): 2026(s), 1989(s), 1954(m), 1910(s), 1880(s).

Reaction of $(Me_2C)(Me_2Si)(t-BuC_5H_3)_2$ (24**) with $Mo(CO)_6$.** A solution of 0.30 g (0.88 mmol) of **24** and 0.60 g (2.27 mmol) of $Mo(CO)_6$ in 30 mL of xylene was refluxed for 6.5 h. After removal of solvent the residue was chromatographed on an alumina column using petroleum ether/ CH_2Cl_2 as eluent. The red band gave 0.07 g (12%) of **25t** as deep red crystals. **25t**: mp 190 °C (dec). Anal. Calcd for $C_{27}H_{30}Mo_2O_6$: C, 50.48; H, 4.71. Found: C, 50.50; H, 4.79. 1H NMR ($CDCl_3$) δ : 5.45 (m, 2H, C_5H_3), 5.10 (m, 2H, C_5H_3), 4.86 (m, 2H, C_5H_3), 1.46 (s, 6H, C-Me), 1.20 (s, 18H, CMe₃). IR (ν_{CO} , cm^{-1}): 2002(s), 1950(s), 1918(w), 1890(s), 1870(s).

Reaction of $(Me_2C)(Me_2Si)(t-BuC_5H_3)_2$ (24**) with $W(CO)_6$.** A solution of 1.00 g (2.94 mmol) of **24** and 1.50 g (4.26 mmol) of $W(CO)_6$ in 40 mL of xylene was refluxed for 24 h. After removal of the solvent the residue was chromatographed on an alumina column using petroleum ether/ CH_2Cl_2 as eluent. The red band gave 0.20 g (8%) of the mixture of **26t** and **26c** as black-red crystals. According to the different crystal shape, a small amount of pure *cis* isomer **26c** and *trans* isomer **26t** were separated mechanically. **26t**: mp 190 °C (dec). Anal. Calcd for $C_{27}H_{30}W_2O_6$: C, 39.63; H, 3.70. Found: C, 39.51; H, 3.63. 1H NMR ($CDCl_3$) δ : 5.52 (m, 2H, C_5H_3), 5.03 (m, 2H, C_5H_3), 4.97 (m, 2H, C_5H_3), 1.50 (s, 3H, C-Me), 1.47 (s, 3H, C-Me), 1.22 (s, 18H, CMe₃). IR (ν_{CO} , cm^{-1}): 2002(s), 1954(s), 1944(s), 1910(s), 1878(s), 1862(s). **26c**: mp 210 °C (dec). Anal.

Calcd for $C_{27}H_{30}Mo_2O_6$: C, 39.63; H, 3.70. Found: C, 39.56; H, 3.65. 1H NMR ($CDCl_3$) δ : 5.28 (m, 6H, C_5H_3), 1.54 (s, 3H, C-Me), 1.49 (s, 3H, C-Me), 1.24 (s, 18H, CMe₃). IR (ν_{CO} , cm^{-1}): 2002(s), 1942(s), 1890(s), 1876(s).

Crystallographic Studies. Single crystals of complexes **2**, **6**, **8**, **10**, **11**, **13**, **14**, **15**, **19**, **21**, **22**, **25t**, and **26t** suitable for X-ray diffraction were obtained from hexane/ CH_2Cl_2 solution. Data collection was performed on a Bruker SMART 1000, using graphite-monochromated Mo K α radiation (ω - 2θ scans, λ = 0.71073 Å). Semiempirical absorption corrections were applied for all complexes. The structures were solved by direct methods and refined by full-matrix least-squares. All calculations were using the SHELXL-97 program system. The crystal data and summary of X-ray data collection are presented in Tables 1 and 2.

Results and Discussion

Reaction of the Carbon and Silicon Doubly Bridged Biscyclopentadiene Ligands with $Mo(CO)_6$. When the carbon and silicon doubly bridged biscyclopentadiene ligands (X)(Y)(C_5H_4)₂ [Y = Me_2Si , X = Me_2C (**1**), (CH_2)₅C (**4**), CH_2 (**9**); Y = Ph_2Si , X = Me_2C (**7**)] reacted with $Mo(CO)_6$ in refluxing xylene, the corresponding intramolecular dimolybdenum complexes (X)(Y)[(η^5 - C_5H_3) $Mo(CO)_3$]₂ [Y = Me_2Si , X = Me_2C (**2**), (CH_2)₅C (**5**), CH_2 (**10**); Y = Ph_2Si , X = Me_2C (**8**)] and the desilylation products (X)[(η^5 - C_5H_4) $Mo(CO)_3$]₂ [X = Me_2C (**3**), (CH_2)₅C (**6**)] were obtained (Scheme 1). The expected complex of type C was not isolated in all cases, although the steric effect at the bridging carbon atom or silicon atom was changed with different substituents. This is different from the reactions of the carbon and silicon doubly bridged biscyclopentadiene ligands with $Fe(CO)_5$, which afforded novel complexes with Fe–Si bonds.^{4b} When the reaction was performed in toluene, similar products were obtained but in lower yields. In DME or diglyme, only the desilylation products were obtained. All these complexes are air stable in the solid state. The doubly bridged biscyclopentadienyl dimolybdenum complexes **2**, **5**, and **8** are slightly air sensitive in solution, which is in agreement with the superlong Mo–Mo bond distances within their molecular structures. All these complexes show two or three Cp–H proton peaks at 5.60–5.07 ppm in the 1H NMR spectra and four to six strong terminal carbonyl bands at 2026–1860 cm^{-1} in the IR spectra. In the 1H NMR spectrum of **10** the bridging methylene protons were split as two double peaks at 3.92, 3.24 ($\Delta\delta$ = 0.68 ppm) with J = 16.0 Hz, which is much greater than that of ligand **9** ($\Delta\delta$: 0.10 ppm),^{4b} and the Si-Me protons were split as two single peaks at 0.57, 0.33 ppm ($\Delta\delta$ = 24 ppm), which is much smaller than that of ligand **9** ($\Delta\delta$: 1.64 ppm).

Reaction of the Carbon and Silicon Doubly Bridged Biscyclopentadiene Ligands with $W(CO)_6$. When the carbon and silicon doubly bridged biscyclopentadiene ligands (X)(Y)(C_5H_4)₂ [Y = Me_2Si , X = Me_2C (**1**), (CH_2)₅C (**4**), CH_2 (**9**); Y = Ph_2Si , X = Me_2C (**7**)] reacted with $W(CO)_6$ in refluxing xylene, novel complexes (X)(η^5 - C_5H_3)(η^5 , η^1 - C_5H_3)[(Y)W(CO)₃][W(CO)₃] [Y = Me_2Si ; X = Me_2C (**13**), (CH_2)₅C (**15**)] (type C) were isolated in addition to the ditungsten complexes (X)(Y)-[(η^5 - C_5H_3)W(CO)₃]₂ [X = Me_2C ; Y = Me_2Si (**11**), Ph_2Si (**16**)] and the desilylation products (X)[(η^5 - C_5H_4)W(CO)₃]₂ [X = Me_2C (**13**), (CH_2)₅C (**15**)] (Scheme 1). All these complexes are air stable except the ditungsten

Table 1. Crystal Data and Summary of X-ray Data Collection of 2, 6, 8, 10, 11, 13–15, 19, and 21

	2	6	8	10	11
formula	C ₂₁ H ₁₈ Mo ₂ O ₆ Si	C ₂₂ H ₁₈ Mo ₂ O ₆	C ₃₁ H ₂₂ Mo ₂ O ₆ Si	C ₁₉ H ₁₄ Mo ₂ O ₆ Si	C ₂₁ H ₁₈ O ₆ SiW ₂
fw	586.32	570.24	710.46	558.27	762.14
cryst syst	monoclinic	monoclinic	monoclinic	monoclinic	monoclinic
space group	<i>P2₁/m</i>	<i>P2₁/c</i>	<i>P2₁/c</i>	<i>P2₁/n</i>	<i>P2₁/n</i>
<i>a</i> (Å)	9.098(3)	13.982(10)	11.352(5)	10.000(3)	9.030(5)
<i>b</i> (Å)	14.337(5)	10.557(8)	15.051(6)	13.870(5)	14.267(9)
<i>c</i> (Å)	9.710(3)	15.492(11)	16.731(7)	14.489(5)	9.649(6)
α (deg)	90	90	90	90	90
β (deg)	117.384(5)	114.687(11)	101.09(3)	96.700(6)	117.500(9)
γ (deg)	90	90	90	90	90
<i>V</i> (Å ³)	1124.5(6)	2078(3)	2805(2)	1996.0(12)	1102.7(11)
<i>Z</i>	2	4	4	4	2
<i>D</i> _{calc} (g·cm ⁻³)	1.732	1.823	1.682	1.858	2.295
μ (mm ⁻¹)	1.202	1.244	0.980	1.349	10.512
<i>F</i> (000)	580	1128	1416	1096	708
cryst size (mm)	0.25 × 0.20 × 0.20	0.26 × 0.24 × 0.20	0.20 × 0.16 × 0.12	0.20 × 0.18 × 0.10	0.24 × 0.22 × 0.20
max. 2θ (deg)	50.04	52.96	50.10	52.82	52.08
no. of reflns collected	4696	11545	8847	9165	5980
no. of indep reflns/ <i>R</i> _{int}	2077/0.0231	4260/0.0334	4888/0.0447	4058/0.0373	2268/0.0501
no. of params	166	271	361	253	146
goodness-of-fit on <i>F</i> ²	1.010	1.009	1.002	0.999	1.040
<i>R</i> ₁ , <i>wR</i> ₂ [<i>I</i> > 2σ(<i>I</i>)]	0.0226, 0.0541	0.0276, 0.0565	0.0411, 0.0974	0.0349, 0.0624	0.0332, 0.0610
<i>R</i> ₁ , <i>wR</i> ₂ (all data)	0.0309, 0.0577	0.0463, 0.0616	0.0830, 0.1137	0.0659, 0.0695	0.0581, 0.0679

	13	14	15	19	21
formula	C ₂₁ H ₁₈ O ₆ SiW ₂	C ₂₂ H ₁₈ O ₆ W ₂	C ₂₄ H ₂₂ O ₆ SiW ₂	C ₂₁ H ₁₈ GeMo ₂ O ₆	C ₂₄ H ₂₂ GeMo ₂ O ₆
fw	762.14	746.06	802.21	630.82	670.89
cryst syst	triclinic	monoclinic	triclinic	triclinic	triclinic
space group	<i>P1</i>	<i>P2(1)/c</i>	<i>P1</i>	<i>P1</i>	<i>P1</i>
<i>a</i> (Å)	9.540(4)	13.915(9)	9.776(3)	9.614(3)	9.770(3)
<i>b</i> (Å)	10.366(5)	10.500(6)	9.764(3)	10.472(4)	9.847(3)
<i>c</i> (Å)	11.167(5)	15.413(9)	13.718(4)	11.189(4)	13.793(5)
α (deg)	101.693(7)	90	76.427(5)	101.361(6)	76.617(6)
β (deg)	93.921(7)	114.273(9)	74.818(5)	94.495(6)	75.152(6)
γ (deg)	92.578(8)	90	69.489(5)	92.575(6)	69.777(5)
<i>V</i> (Å ³)	1077.0(8)	2053(2)	1168.7(6)	1099.0(7)	1188.6(7)
<i>Z</i>	2	4	2	2	2
<i>D</i> _{calc} (g·cm ⁻³)	2.350	2.414	2.280	1.906	1.875
μ (mm ⁻¹)	10.763	11.235	9.925	2.517	2.333
<i>F</i> (000)	708	1384	752	616	660
cryst size (mm)	0.20 × 0.16 × 0.12	0.22 × 0.20 × 0.18	0.24 × 0.22 × 0.16	0.24 × 0.22 × 0.18	0.20 × 0.16 × 0.08
max. 2θ (deg)	50.00	53.00	52.84	52.84	52.84
no. of reflns collected	5641	11554	6762	6275	6917
no. of indep reflns/ <i>R</i> _{int}	3787/0.0405	4164/0.0800	4745/0.0605	4423/0.0295	4803/0.0285
no. of params	276	271	301	272	301
goodness-of-fit on <i>F</i> ²	0.972	0.940	0.975	0.998	1.002
<i>R</i> ₁ , <i>wR</i> ₂ [<i>I</i> > 2σ(<i>I</i>)]	0.0391, 0.0686	0.0404, 0.0658	0.0568, 0.1243	0.0376, 0.0762	0.0325, 0.0627
<i>R</i> ₁ , <i>wR</i> ₂ (all data)	0.0714, 0.0776	0.0838, 0.0757	0.0920, 0.1397	0.0689, 0.0858	0.0576, 0.0723

complexes **11** and **16**, which are slightly air sensitive especially in solution. The IR spectra of **13** and **15** exhibited five terminal carbonyl bands at 2026, 1989, 1940, 1914, 1890 cm⁻¹ and 2026, 1989, 1940, 1914, 1890 cm⁻¹, respectively. Their ¹H NMR spectra displayed six or five Cp-H proton peaks at 6.20, 5.84, 5.30, 5.19, 5.10, 4.96 and 6.31, 5.85, 5.27 (2H), 5.10, 4.95 ppm, respectively, indicating the unsymmetrical structures. X-ray diffraction analysis shows that complexes **13** and **15** contain a W–Si bond, suggesting that the formation of **13** and **15** should be accompanied by the cleavage of a C–Si bond in the ligands. The structures of **13** and **15** are very similar to the complexes (X)(η⁵-C₅H₃)(η⁵,η¹-C₅H₃)[(Me₂Si)Fe(CO)₂][Fe(CO)₂] [X = Me₂C, (CH₂)₅C],^{4b} which were obtained from the reactions of the corresponding ligands with Fe(CO)₅ in refluxing xylene.

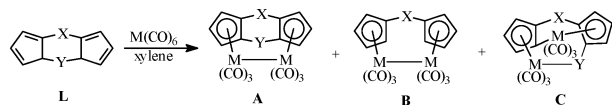
The reaction of ligand **4** with W(CO)₆ only gave type C complex **15** and the desilylation product **14**. The corresponding ditungsten complex was not isolated. On the other hand, the reaction of ligand **7** gave only ditungsten complex **16** and the desilylation product **12**. No type C complex was obtained. This indicates, similar

to the reaction with Fe(CO)₅, that the bulky substituents at the bridging carbon atom may promote the formation of the complex of type C, whereas the two phenyl groups at the bridging silicon atom may prevent the formation of the complex of type C. It was noteworthy that the reaction of ligand **9** with W(CO)₆ gave the desilylation product **17** as the only isolable product.

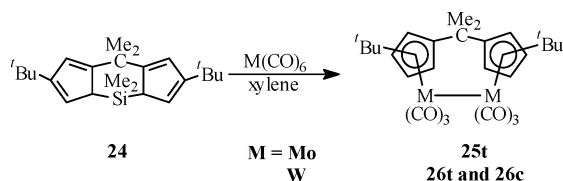
Reaction of the Carbon and Germanium Doubly Bridged Biscyclopentadiene Ligands with M(CO)₆ (M = Mo, W). When the carbon and germanium doubly bridged biscyclopentadiene ligands (X)(Me₂Ge)(C₅H₄)₂ [X = Me₂C (**18**), (CH₂)₅C (**20**)] reacted with Mo(CO)₆ or W(CO)₆, similar novel complexes of type C, (X)(η⁵-C₅H₃)(η⁵,η¹-C₅H₃)[(Me₂Ge)M(CO)₃][M(CO)₃] [M = Mo, X = Me₂C (**19**), (CH₂)₅C (**21**); M = W, X = Me₂C (**22**), (CH₂)₅C (**23**)], were obtained along with the degermylation products (Scheme 1). However in this case, the corresponding dimolybdenum or ditungsten complexes were not isolated, probably due to the weakness of the C–Ge bond. All the isolated complexes are air stable. The ¹H NMR spectra of **19**, **21**, **22**, and **23** each displayed six Cp-H proton peaks at 6.30–4.90 ppm,

Table 2. Crystal Data and Summary of X-ray Data Collection for **22**, **25t**, and **26t**

	22	25t	26t
formula	C ₂₁ H ₁₈ GeO ₆ W ₂	C ₂₇ H ₃₀ Mo ₂ O ₆	C ₂₇ H ₃₀ O ₆ W ₂
fw	806.64	642.39	818.21
cryst syst	triclinic	monoclinic	monoclinic
space group	<i>P</i> $\bar{1}$	<i>P2</i> ₁ / <i>c</i>	<i>P2</i> ₁ / <i>c</i>
<i>a</i> (Å)	9.546(3)	16.530(7)	16.498(19)
<i>b</i> (Å)	10.398(4)	9.453(4)	9.435(11)
<i>c</i> (Å)	11.104(4)	19.501(8)	19.45(2)
α (deg)	101.448(5)	90	90
β (deg)	94.525(6)	114.838(6)	114.672(16)
γ (deg)	92.555(5)	90	90
<i>V</i> (Å ³)	1074.8(6)	2765(2)	2751(5)
<i>Z</i>	2	4	4
<i>D</i> _{calc} (g·cm ⁻³)	2.493	1.543	1.976
μ (mm ⁻¹)	12.101	0.944	8.393
<i>F</i> (000)	744	1296	1552
cryst size (mm)	0.32 × 0.24 × 0.20	0.34 × 0.26 × 0.22	0.26 × 0.22 × 0.20
max. 2 θ (deg)	50.00	52.80	52.86
no. of reflns collected	5383	12633	15114
no. of indep reflns/ <i>R</i> _{int}	3686/0.0325	5584/0.0447	5590/0.0501
no. of params	276	317	324
goodness-of-fit on <i>F</i> ²	0.997	1.026	1.040
<i>R</i> ₁ , <i>wR</i> ₂ [<i>I</i> > 2 σ (<i>I</i>)]	0.0414, 0.1012	0.0402, 0.0693	0.0389, 0.0847
<i>R</i> ₁ , <i>wR</i> ₂ (all data)	0.0565, 0.1097	0.0822, 0.0788	0.0685, 0.0947

Scheme 1

X	Y	M	L	A	B	C
Me ₂ C	Me ₂ Si	Mo	1	2	3	
(CH ₂) ₃ C	Me ₂ Si	Mo	4	5	6	
Me ₂ C	Ph ₂ Si	Mo	7	8	3	
CH ₂	Me ₂ Si	Mo	9	10		
Me ₂ C	Me ₂ Si	W	1	11	12	13
(CH ₂) ₃ C	Me ₂ Si	W	4	4	14	15
Me ₂ C	Ph ₂ Si	W	7	16	12	
CH ₂	Me ₂ Si	W	9		17	
Me ₂ C	Me ₂ Ge	Mo	18		3	19
(CH ₂) ₃ C	Me ₂ Ge	Mo	20		6	21
Me ₂ C	Me ₂ Ge	W	18		12	22
(CH ₂) ₃ C	Me ₂ Ge	W	20		14	23

Scheme 2

suggesting again the unsymmetrical structures. Moreover, we already noted that the reactions of **1** and **4**, silyl analogues of **18** and **20**, failed to give any type C complexes. The formation of type C molybdenum complexes **19** and **21** here indicates that the weaker C–Ge bond favors the formation of type C structure through the cleavage of the C–Ge bond.

Reaction of (Me₂C)(Me₂Si)(*t*-BuC₅H₃)₂ (24**) with M(CO)₆ (M = Mo, W).** To study the steric effect of this reaction, a *tert*-butyl group was introduced to the cyclopentadienyl rings and the ligand (Me₂C)(Me₂Si)(*t*-BuC₅H₃)₂ (**24**) was used in the reaction. However, when **24** reacted with Mo(CO)₆ or W(CO)₆ under refluxing

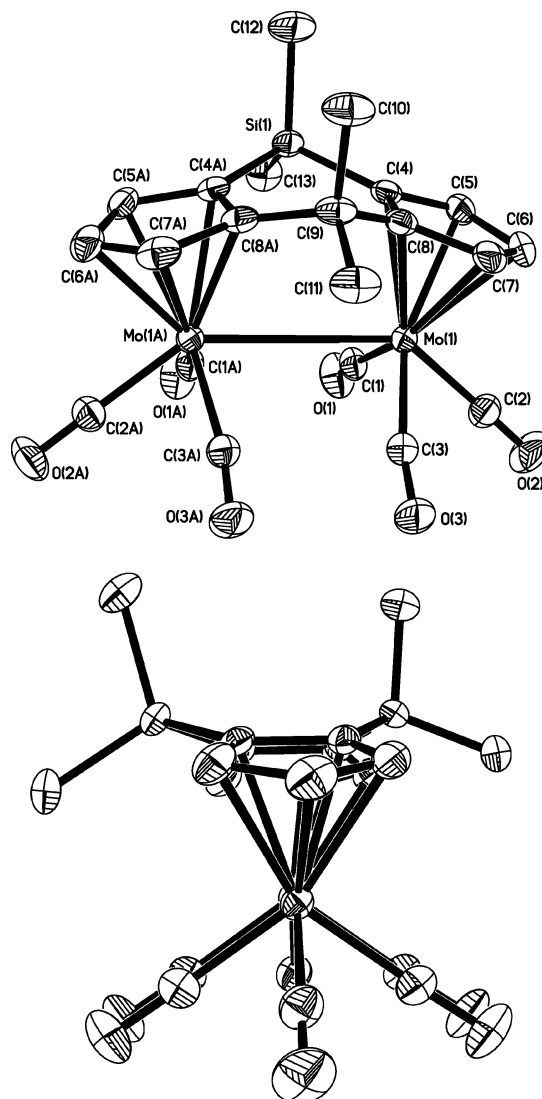


Figure 1. ORTEP diagram of **2**. Thermal ellipsoids are shown at the 30% level. The top drawing shows the view perpendicular to the Mo–Mo bond and the labeling scheme. The bottom drawing depicts the view down the Mo–Mo axis. Selected bond lengths [Å] and angles [deg]: Mo(1)–Mo(1a) 3.4328(12), Mo(1)–C(4) 2.341(3), Mo(1)–C(8) 2.347(3), Si(1)–C(4) 1.858(3), C(8)–C(9) 1.515(3), C(4a)–Si(1)–C(4) 96.33(17), O(1)–C(1)–Mo(1) 169.8(3), O(2)–C(2)–Mo(1) 179.2(3), O(3)–C(3)–Mo(1) 170.0(3), C(8)–C(9)–C(8a) 109.4(3).

xylene, only the desilylation products **25** and **26** were obtained (Scheme 2).

Neither the normal intramolecular dinuclear complex (type A) nor the type C complex was obtained. The bulky *tert*-butyl groups might either prevent the formation of the type C complex and/or promote the desilylation reaction. Both the *cis* (two *tert*-butyl groups on the same side) and *trans* (two *tert*-butyl groups on opposite sides) isomers of **26** were obtained, but only one isomer of **25** was isolated and assigned to the *trans* isomer **25t** based on the X-ray diffraction analysis.

Molecular Structures. The molecular structures of **2**, **6**, **8**, **10**, **11**, **13**, **14**, **15**, **19**, **21**, **22**, **25t**, and **26t** are shown in Figures 1–13, respectively.

Complexes **2**, **8**, **10**, and **11** are intramolecular doubly bridged bicyclopentadienyl dimolybdenum or ditungsten complexes. The M–M distances in complexes **2**

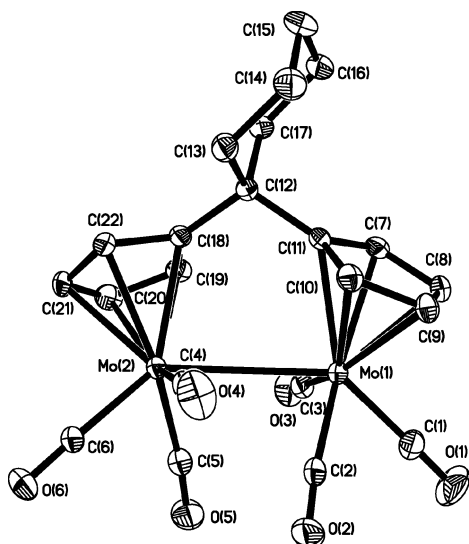


Figure 2. ORTEP diagram of **6**. Thermal ellipsoids are shown at the 30% level. Selected bond lengths [Å] and angles [deg]: Mo(1)–Mo(2) 3.1708(18), Mo(1)–C(11) 2.415(3), Mo(2)–C(18) 2.367(3), C(11)–C(12) 1.531(4), C(12)–C(18) 1.525(4), C(11)–Mo(1)–Mo(2) 80.20(7), C(18)–Mo(2)–Mo(1) 81.68(7), C(12)–C(11)–Mo(1) 129.89(18), C(18)–C(12)–C(11) 111.8(2), C(12)–C(18)–Mo(2) 126.93(19).

[3.4328(12) Å], **8** [3.453(2) Å], and **11** [3.403(2) Å] are conspicuously elongated and are in fact the longest ever reported among the biscyclopentadienyl dimolybdenum or ditungsten complexes (Table 3). The covalent radius of the molybdenum atom has been estimated from structural data of Mo(dien)(CO)₃ to be 1.62 Å.^{8,9} So the distances of the Mo–Mo bond in complexes **2** [3.4328(12) Å] and **8** [3.453(2) Å] are on average 0.2 Å greater than the sum of the covalent radius of two molybdenum (3.24 Å). This is very different from the singly bridged biscyclopentadienyl dimolybdenum or ditungsten complexes, in which cases the bridging caused a small decrease in the M–M distances. This can be attributed to three factors. First, the inflexibility of the doubly bridged biscyclopentadienyl dinuclear metal complexes forces the CO groups on the different metal atoms to repel each other and thereby increases the M–M distance. In singly bridged biscyclopentadienyl dimolybdenum or ditungsten complexes, the flexibility of the singly bridged biscyclopentadienyl ligands could reduce the above-mentioned repulsion by increasing the CNT–M–M–CNT' (CNT = centroid of cyclopentadienyl ring) torsion angles. The structures of complexes **2**, **8**, and **11** are conformationally much more rigid and constrained as a result of the double bridges. The CNT–M–M–CNT' torsion angles for the doubly bridged complexes (0° for **2**, 1.7° for **8**, 0° for **11**) are much smaller than those in the singly bridged complexes (44–48°). As a result of such constrained structures, the repulsion between the CO groups on the different metal atoms will be much greater than that in the singly bridged complexes if the M–M bond remains the same length. In these bridged complexes, a relationship appears to exist between the degree of twist in a molecule and its M–M distance (Table 3). In general,

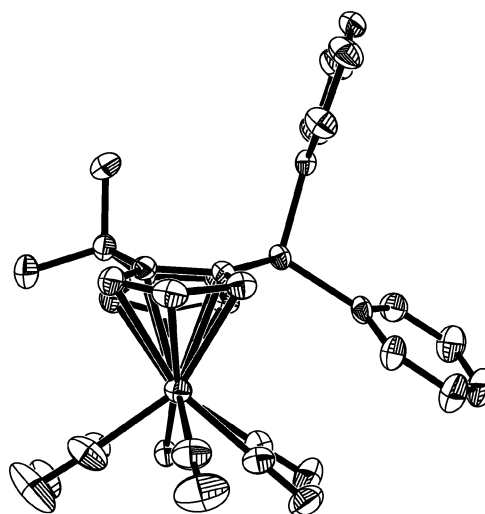
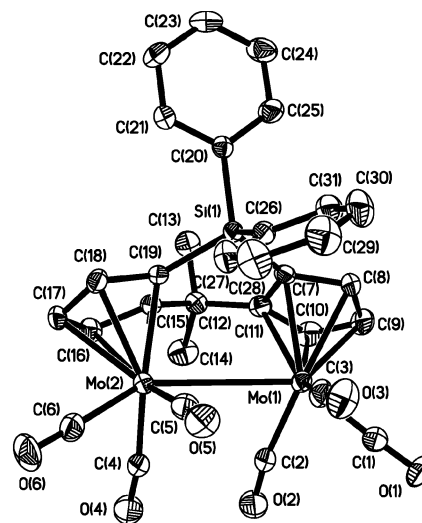


Figure 3. ORTEP diagram of **8**. Thermal ellipsoids are shown at the 30% level. The top drawing shows the view perpendicular to the Mo–Mo bond and the labeling scheme. The bottom drawing depicts the view down the Mo–Mo axis. Selected bond lengths [Å] and angles [deg]: Mo(1)–Mo(2) 3.453(2), Mo(1)–C(7) 2.335(6), Mo(1)–C(11) 2.346(6), Mo(2)–C(15) 2.365(6), Mo(2)–C(19) 2.323(5), Si(1)–C(7) 1.855(6), Si(1)–C(19) 1.853(6), C(11)–C(12) 1.515(8), C(12)–C(15) 1.533(8), C(19)–Si(1)–C(7) 98.8(3), C(20)–Si(1)–C(26) 107.4(3), C(11)–C(12)–C(15) 109.7(5), O(1)–C(1)–Mo(1) 177.8(6), O(2)–C(2)–Mo(1) 168.3(6), O(3)–C(3)–Mo(1) 170.0(6), O(4)–C(4)–Mo(2) 172.0(6), O(5)–C(5)–Mo(2) 170.6(6), O(6)–C(6)–Mo(2) 177.9(6).

the M–M distances increase with decreasing CNT–M–M–CNT' torsion angles (except **10**). Second, all these complexes contain single carbon and single silicon atom double bridges, which are the shortest bridges for the doubly bridged biscyclopentadienyl metal complexes up to now. Such short bridges increase the steric repulsions between the substituents at two bridge atoms and the substituents with Mo(CO)₃ groups, which make the ∠Cp–Cp fold angle (149.3° for **2**, 149.5° for **8**, 149.2° for **11**) much larger than those with two longer bridges (for example, (Me₂Si)₂[C₅H₃W(CO)₃]₂¹² 135.6°) or singly

(8) Cotton, F. A. And Wing, R. M. *Inorg. Chem.* **1965**, *4*, 314.

(9) Adams, R. D.; Collins, D. M.; Cotton, F. A. *J. Am. Chem. Soc.* **1974**, *96*, 749.

(10) Adams, R. D.; Collins, D. M.; Cotton, F. A. *Inorg. Chem.* **1974**, *13*, 1086.

(11) Drage, J. S.; Vollhardt, K. P. *Organometallics* **1986**, *5*, 280.

(12) McKinley, S. G.; Angelici, R. J.; Choi, M.-G. *Organometallics* **2002**, *21*, 1235.

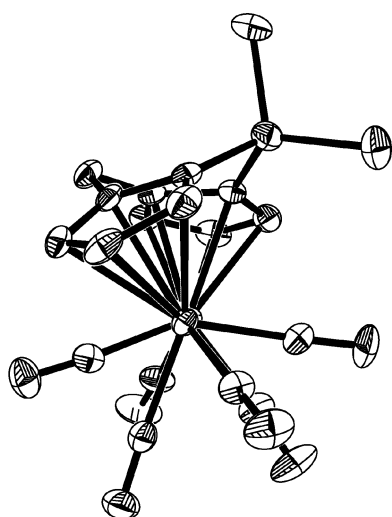
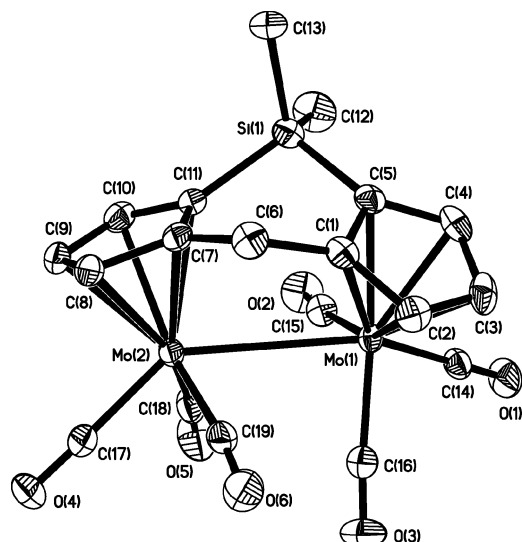


Figure 4. ORTEP diagram of **10**. Thermal ellipsoids are shown at the 30% level. The top drawing shows the view perpendicular to the Mo–Mo bond and the labeling scheme. The bottom drawing depicts the view down the Mo–Mo axis. Selected bond lengths [Å] and angles [deg]: Mo(1)–Mo(2) 3.1669(9), Mo(1)–C(1) 2.426(4), Mo(1)–C(5) 2.353(4), Mo(2)–C(7) 2.303(4), Mo(2)–C(11) 2.409(4), Si(1)–C(5) 1.876(4), Si(1)–C(11) 1.889(4), C(1)–C(6) 1.513(5), C(6)–C(7) 1.513(5), C(5)–Si(1)–C(11) 97.32(18), C(7)–C(6)–C(1) 111.6(3).

bridged biscyclopentadienyl dimolybdenum (or ditungsten) complexes ($\sim 120^\circ$) (Table 3), and thus lead to increased M–M distances. Third, the bridging carbon and silicon atom each is substituted with two methyl or phenyl groups. The steric repulsions between the substituents at the two bridge atoms and the $M(\text{CO})_3$ moiety again make the $\angle\text{Cp}–\text{Cp}$ fold angle (149.3° in **2**, 149.5° in **8**, 149.2° in **11**) much larger than the unsubstituted analogues (for example, $(\text{CH}_2)(\text{Me}_2\text{Si})[(\eta^5\text{-C}_5\text{H}_3)\text{Mo}(\text{CO})_3]_2$ (**10**), 133.7°) and therefore favor forming structures with longer M–M distances. It is interesting that the $\angle\text{Cp}–\text{Cp}$ fold angles in **2**, **8**, and **11** are comparable with that in $(\text{Me}_2\text{Si})_2[\text{C}_5\text{H}_3\text{W}(\text{CO})_3]_2\text{H}^+$ [$149.7(2)^\circ$],¹² which has long a $\text{W}\cdots\text{W}$ distance [3.657(6) Å] without bonding. Further studies on the effects of the long M–M distances on the reactivity of these

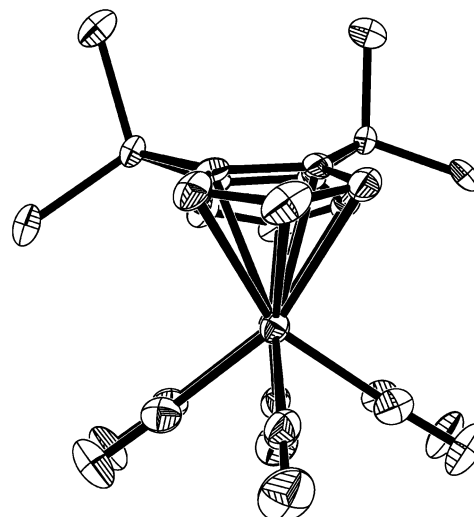
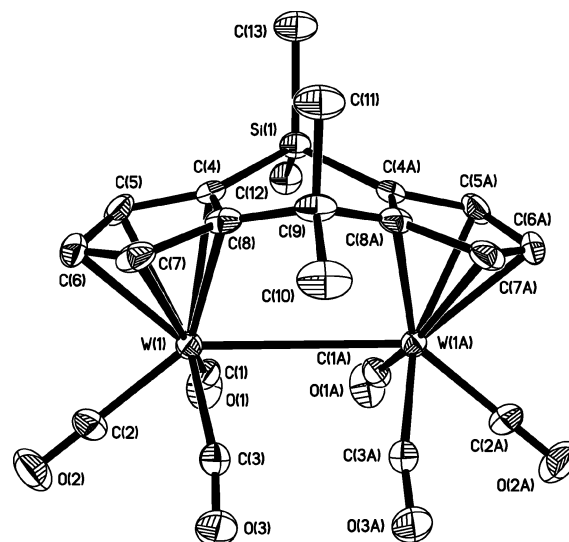


Figure 5. ORTEP diagram of **11**. Thermal ellipsoids are shown at the 30% level. The top drawing shows the view perpendicular to the Mo–Mo axis. Selected bond lengths [Å] and angles [deg]: W(1)–W(1a) 3.403(2), W(1)–C(4) 2.328(6), W(1)–C(8) 2.331(7), Si(1)–C(4) 1.838(8), C(8)–C(9) 1.515(10), C(4a)1–Si(1)–C(4) $95.9(5)$, O(1)–C(1)–W(1) $171.0(7)$, O(2)–C(2)–W(1) $179.3(8)$, O(3)–C(3)–W(1) $169.3(7)$, C(8)–C(9)–C(8a) $110.1(8)$.

complexes are being continued in our laboratories. The molecule of complex **10** has no substituent at the bridging carbon atom. In this case the intramolecular nonbonding interaction was remarkably reduced, as reflected by a decreased $\angle\text{Cp}–\text{Cp}$ fold angle (133.7°) and shortened Mo–Mo bond distance. It is interesting that complex **10** has a slightly shorter Mo–Mo distance [3.1669(9) Å] even than some singly bridged biscyclopentadienyl dinuclear metal complexes [3.1708(18) Å for **6**, 3.1723(11) Å for **25t**], although its $\angle\text{Cp}–\text{Cp}$ fold angle and the $\text{CNT}–\text{Mo}–\text{Mo}–\text{CNT}'$ torsion angle (34.0°) are between those of the doubly bridged and singly bridged biscyclopentadienyl dimolybdenum complexes. This may be attributed to the considerably reduced steric effect of the CH_2 bridge as noted previously in the singly CH_2 bridged complex $\text{CH}_2[\text{C}_5\text{H}_4\text{Mo}(\text{CO})_3]_2$ (Mo–Mo 3.1406 Å).⁶

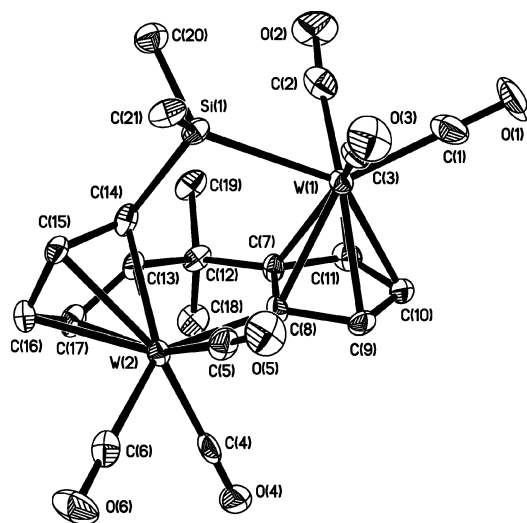


Figure 6. ORTEP diagram of **13**. Thermal ellipsoids are shown at the 30% level. Selected bond lengths [Å] and angles [deg]: W(1)–Si(1) 2.620(3), W(1)–C(7) 2.315(10), W(1)–C(8) 2.368(10), W(2)–C(8) 2.225(9), W(2)–C(13) 2.306(9), W(2)–C(14) 2.286(11), Si(1)–C(14) 1.922(11), C(7)–C(12) 1.544(13), C(12)–C(13) 1.527(13), C(7)–W(1)–Si(1) 85.9(2), C(8)–W(1)–Si(1) 83.4(2), C(8)–W(2)–C(13) 73.3(3), C(8)–W(2)–C(14) 80.7(3), C(14)–Si(1)–W(1) 104.1(3), W(2)–C(8)–W(1) 128.7(4), C(13)–C(12)–C(7) 104.9(7).

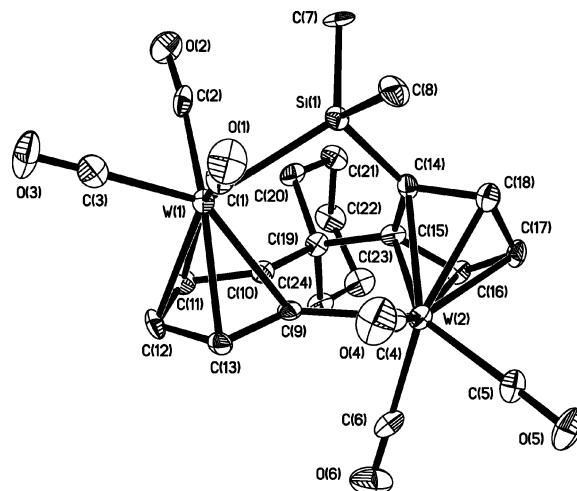


Figure 8. ORTEP diagram of **15**. Thermal ellipsoids are shown at the 30% level. Selected bond lengths [Å] and angles [deg]: W(1)–Si(1) 2.617(3), W(1)–C(9) 2.378(11), W(1)–C(10) 2.326(13), W(2)–C(9) 2.221(12), W(2)–C(14) 2.306(11), W(2)–C(15) 2.336(12), Si(1)–C(14) 1.911(14), C(10)–C(19) 1.522(17), C(15)–C(19) 1.540(17), C(9)–W(1)–Si(1) 84.1(3), C(10)–W(1)–Si(1) 86.3(3), C(9)–W(2)–C(14) 81.2(4), C(9)–W(2)–C(15) 74.2(5), C(14)–Si(1)–W(1) 103.8(4), W(2)–C(9)–W(1) 127.5(5), C(10)–C(19)–C(15) 105.4(10).

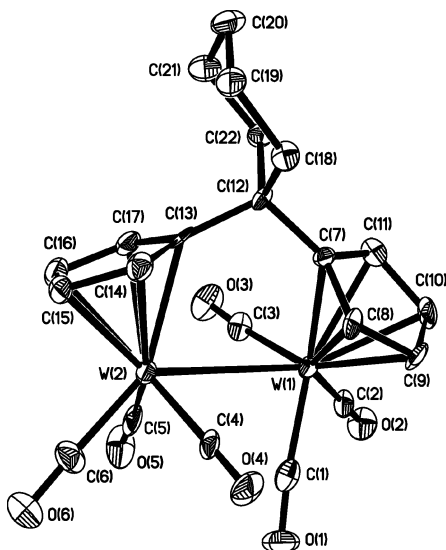


Figure 7. ORTEP diagram of **14**. Thermal ellipsoids are shown at the 30% level. Selected bond lengths [Å] and angles [deg]: W(1)–W(2) 3.1582(16), W(1)–C(7) 2.350(8), W(2)–C(13) 2.404(9), C(7)–C(12) 1.506(11), C(12)–C(13) 1.528(12), C(7)–W(1)–W(2) 81.6(2), C(13)–W(2)–W(1) 80.2(2), C(12)–C(7)–W(1) 127.9(6), C(7)–C(12)–C(13) 111.9(7), C(12)–C(13)–W(2) 129.6(5).

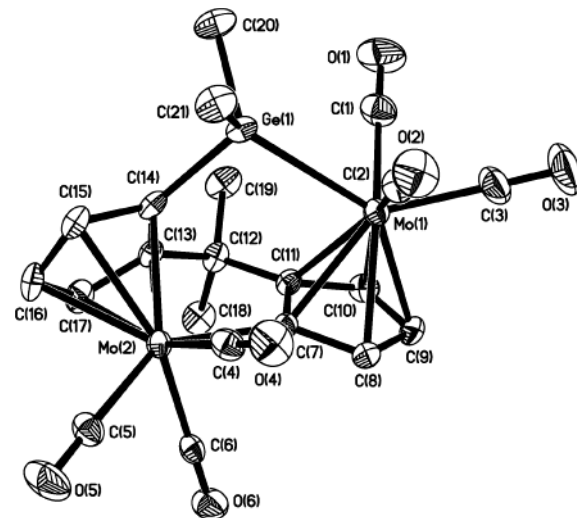


Figure 9. ORTEP diagram of **19**. Thermal ellipsoids are shown at the 30% level. Selected bond lengths [Å] and angles [deg]: Mo(1)–Ge(1) 2.6671(10), Mo(1)–C(7) 2.391(5), Mo(1)–C(8) 2.336(5), Mo(2)–C(7) 2.229(5), Mo(2)–C(13) 2.316(5), Mo(2)–C(14) 2.312(5), Ge(1)–C(14) 1.970(5), C(8)–C(12) 1.522(7), C(12)–C(13) 1.530(7), C(7)–Mo(1)–Ge(1) 83.47(11), C(8)–Mo(1)–Ge(1) 85.35(11), C(7)–Mo(2)–C(13) 73.67(16), C(7)–Mo(2)–C(14) 81.04(17), C(14)–Ge(1)–Mo(1) 103.18(13), Mo(2)–C(7)–Mo(1) 129.4(2), C(8)–C(12)–C(13) 105.1(4).

Complexes **6** and **25t** are singly bridged biscyclopentadienyl dimolybdenum complexes. As shown in Figure 12, **25t** is a *trans* isomer. The Mo–Mo distances are 3.1708(18) Å in **6** and 3.1723(11) Å in **25t**, both shorter than that in *trans*-[CpMo(CO)₃]₂ [3.235(1) Å],¹⁰ showing a moderate compression on the Mo–Mo bond imposed by the single carbon bridged ligand, similar to that in (CH₂)[(η⁵-C₅H₄)Mo(CO)₃]₂ [3.1406 Å].⁶ This may be attributed to the flexibility of the singly bridged biscyclopentadienyl ligands which allows the CO groups to

reduce steric repulsions that force the metal atoms away from each other (CNT–Mo–Mo–CNT torsion angle: 46.4° for **6**, 44.8° for **25t**). For the singly carbon bridged complexes **6** and **25t**, the crowdedness around the Mo–Mo bond is partially relaxed by the assumption of larger CNT–Mo–Mo–CNT torsion angles, which is not possible for the fulvalene complex FvMo₂(CO)₆ and the doubly bridged biscyclopentadienyl complexes **2** and **8** (whose CNT–Mo–Mo–CNT torsion angles were 0° and 1.7°, respectively). Similarly, complexes **14** and **26t** are

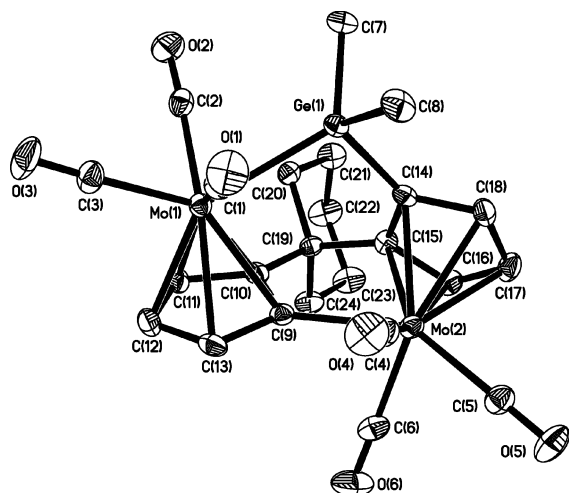


Figure 10. ORTEP diagram of **21**. Thermal ellipsoids are shown at the 30% level. Selected bond lengths [Å] and angles [deg]: Mo(1)–Ge(1) 2.6569(9), Mo(1)–C(9) 2.395(4), Mo(1)–C(10) 2.342(4), Mo(2)–C(9) 2.237(4), Mo(2)–C(14) 2.321(4), Mo(2)–C(15) 2.322(4), Ge(1)–C(14) 1.967(4), C(15)–C(19) 1.518(6), C(10)–C(19) 1.521(5), C(9)–Mo(1)–Ge(1) 84.15(10), C(10)–Mo(1)–Ge(1) 86.13(10), C(9)–Mo(2)–C(14) 81.41(14), C(9)–Mo(2)–C(15) 73.27(14), C(14)–Ge(1)–Mo(1) 103.15(11), Mo(2)–C(9)–Mo(1) 127.72(17), C(15)–C(19)–C(10) 105.6(3).

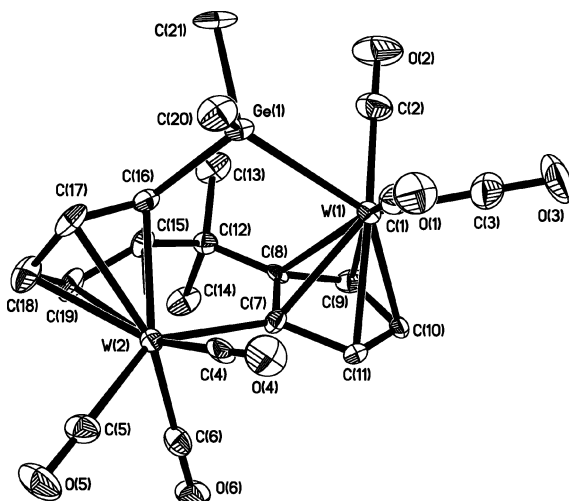


Figure 11. ORTEP diagram of **22**. Thermal ellipsoids are shown at the 30% level. Selected bond lengths [Å] and angles [deg]: W(1)–C(7) 2.370(11), W(1)–C(8) 2.315(9), W(1)–Ge(1) 2.6522(13), W(2)–C(7) 2.213(10), W(2)–C(15) 2.308(10), W(2)–C(16) 2.289(10), Ge(1)–C(16) 1.982(11), C(8)–C(12) 1.502(13), C(12)–C(15) 1.493(14), C(7)–W(1)–Ge(1) 83.5(2), C(8)–W(1)–Ge(1) 85.3(2), C(7)–W(2)–C(15) 73.1(3), C(7)–W(2)–C(16) 81.4(4), C(16)–Ge(1)–W(1) 103.3(3), W(2)–C(7)–W(1) 129.5(4), C(15)–C(12)–C(8) 106.1(8).

singly bridged biscyclopentadienyl ditungsten complexes. **26t** is a *trans* isomer, as shown in Figure 13. Similar to $(\text{CH}_2)[(\eta^5\text{-C}_5\text{H}_4)\text{W}(\text{CO})_3]_2$ [3.166(1) Å],⁷ the W–W distances in **14** [3.1582(16) Å] and **26t** [3.165(3) Å], as compared to those in nonbridged complex *trans*-($\eta^5\text{-C}_5\text{H}_5$)₂W₂(CO)₆ [3.222(1) Å]¹⁰ and singly silyl bridged complex $(\text{Me}_2\text{Si})(\eta^5\text{-C}_5\text{H}_4)\text{W}(\text{CO})_3]_2$ [3.196(1) Å],¹³ were compressed by the short single carbon bridged ligands. The CNT–W–W–CNT torsion angles are 45.3° for **14**

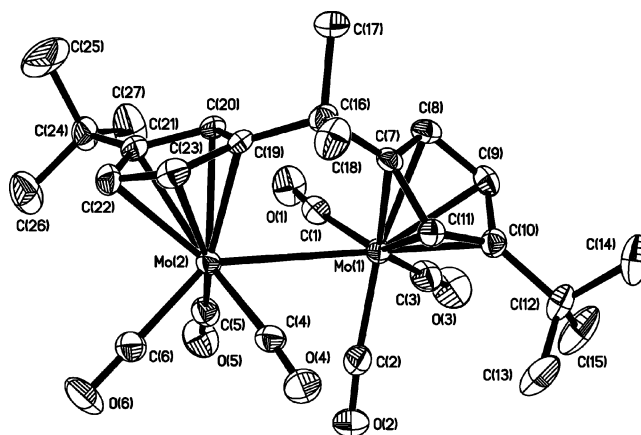


Figure 12. ORTEP diagram of **25t**. Thermal ellipsoids are shown at the 30% level. Selected bond lengths [Å] and angles [deg]: Mo(1)–Mo(2) 3.1723(11), Mo(1)–C(7) 2.401(4), Mo(2)–C(19) 2.328(4), C(7)–C(16) 1.517(5), C(16)–C(19) 1.516(5), C(7)–Mo(1)–Mo(2) 79.43(10), C(19)–Mo(2)–Mo(1) 82.03(10), C(16)–C(7)–Mo(1) 129.6(3), C(19)–C(16)–C(7) 112.8(3), C(16)–C(19)–Mo(2) 125.7(2).

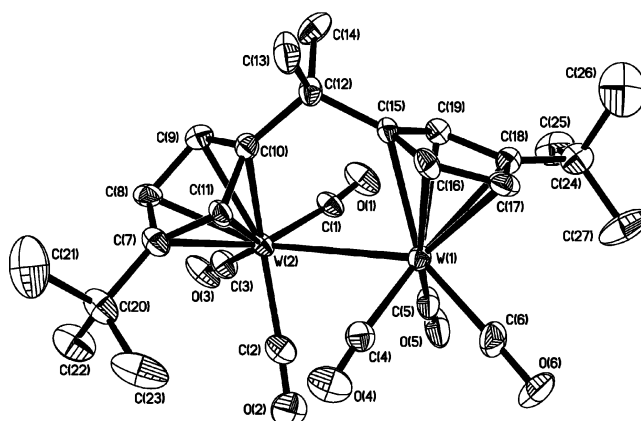


Figure 13. ORTEP diagram of **26t**. Thermal ellipsoids are shown at the 30% level. Selected bond lengths [Å] and angles [deg]: W(1)–W(2) 3.165(3), W(1)–C(15) 2.392(8), W(2)–C(10) 2.321(8), C(10)–C(12) 1.532(10), C(12)–C(15) 1.513(12), C(15)–W(1)–W(2) 79.5(2), C(10)–W(2)–W(1) 82.2(2), C(12)–C(10)–W(2) 125.2(5), C(15)–C(12)–C(10) 112.9(6), C(12)–C(15)–W(1) 129.8(5).

and 47.0° for **26t**, reflecting the flexibility of the singly bridged biscyclopentadienyl ligands.

Complex **13**, **15**, **19**, **21**, and **22** have similar novel structures. These complexes all contain a M–Si or M–Ge bond, and one metal atom is coordinated with a cyclopentadienyl ligand in η^5 manner, while the other metal atom coordinated with both cyclopentadienyl ligands in a η^1 and η^5 manner, respectively. Similar ruthenium complexes $[\text{Ru}(\text{CO})_2]_2(\mu\text{-}\eta^5\text{-}\eta^1\text{-C}_5\text{H}_4)[\mu\text{-Me}_2\text{Si}(\eta^5\text{-C}_5\text{H}_4)]^{15}$ and $[\text{Ru}(\text{CO})_2]_2(\mu\text{-}\eta^5\text{-}\eta^1\text{-C}_5\text{Me}_4)[\mu\text{-Me}_2\text{Si}(\eta^5\text{-C}_5\text{H}_4)]^{16}$ have been reported from the photolysis of silyl-bridged complexes $\text{Me}_2\text{Si}[\eta^5\text{-C}_5\text{H}_4\text{Ru}(\text{CO})_2]_2$ and $\text{Me}_2\text{Si}[\eta^5\text{-C}_5\text{Me}_4\text{Ru}(\text{CO})_2]_2$, respectively. In our recent work, iron complexes $(\text{R}_2\text{C})(\eta^5\text{-C}_5\text{H}_3)(\eta^5, \eta^1\text{-C}_5\text{H}_3)[(\text{Me}_2\text{E})\text{Fe}(\text{CO})_2]_2$ [$\text{R}_2\text{C} = \text{Me}_2\text{C}, (\text{CH}_2)_5\text{C}, \text{E} = \text{Si}, \text{Ge}$] with

(14) Abrahamson, H. B.; Heeg, M. J. *Inorg. Chem.* **1984**, *23*, 2281.

(15) (a) Bitterwolf, T. E.; Shade, J. E.; Hansen, J. A.; Rheingold, A. L. *J. Organomet. Chem.* **1996**, *514*, 13. (b) Bitterwolf, T. E.; Leonard, M. B.; Horine, P. A.; Shade, J. E.; Hansen, J. A.; Rheingold, A. L.; Staley, D. J.; Yap, G. P. A. *J. Organomet. Chem.* **1996**, *512*, 11.

(16) Fox, T.; Burger, P. *Eur. J. Inorg. Chem.* **2001**, 795.

(13) Abriel, W.; Heck, J. J. *Organomet. Chem.* **1986**, *302*, 363.

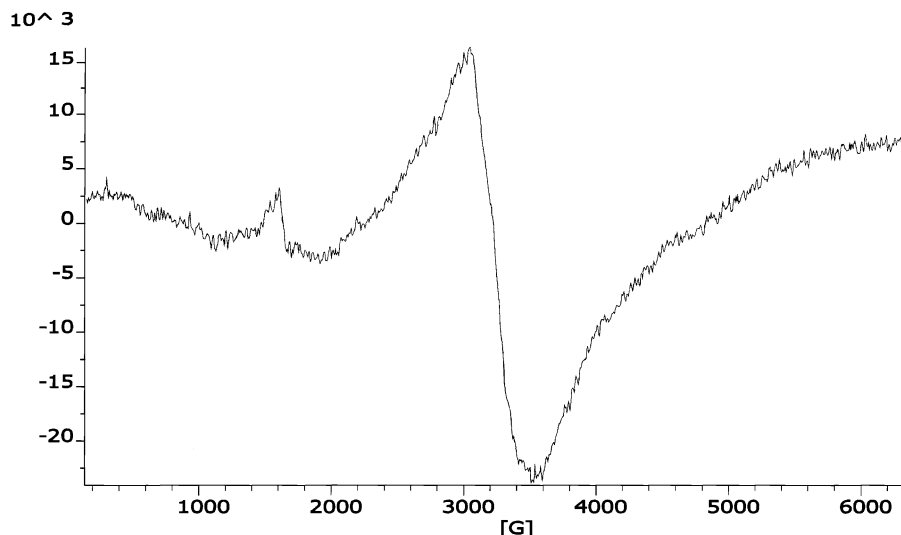


Figure 14. EPR spectrum of **2** in crystal powder.

Table 3. Structural Parameter Comparison for Biscyclopentadienyl Dimolybdenum (Ditungsten) Complexes^a

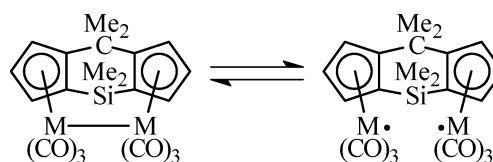
complex	M–M (Å)	∠Cp–Cp fold angle (deg)	CEN–M–M–CEN torsion angles	ref
<i>trans</i> -[CpMo(CO) ₃] ₂	3.235(1)			10
FvMo ₂ (CO) ₆	3.371(1)	164.7		11
CH ₂ [C ₅ H ₄ Mo(CO) ₃] ₂	3.1406			6
(CH ₂) ₅ C[C ₅ H ₄ Mo(CO) ₃] ₂ (6)	3.1708(18)	120.5	46.4	this work
Me ₂ C[<i>t</i> -BuC ₅ H ₃ Mo(CO) ₃] ₂ (25t)	3.1723(11)	121.9	44.8	this work
(Me ₂ C)(Me ₂ Si)[C ₅ H ₃ Mo(CO) ₃] ₂ (2)	3.4328(12)	149.3	0	this work
(Me ₂ C)(Ph ₂ Si)[C ₅ H ₃ Mo(CO) ₃] ₂ (8)	3.453(2)	149.5	1.7	this work
(CH ₂)(Me ₂ Si)[C ₅ H ₃ Mo(CO) ₃] ₂ (10)	3.1669(9)	133.7	34.0	this work
<i>trans</i> -[CpW(CO) ₃] ₂	3.222(1)			10
FvW ₂ (CO) ₆	3.347(1)	163.9	5.0(2)	14
CH ₂ [C ₅ H ₄ W(CO) ₃] ₂	3.166(1)		47.8(6)	7
Me ₂ Si[C ₅ H ₄ W(CO) ₃] ₂	3.196(1)		~47.8	13
(CH ₂) ₅ C[C ₅ H ₄ W(CO) ₃] ₂ (14)	3.1582(16)	120.4	45.3	this work
Me ₂ C[<i>t</i> -BuC ₅ H ₃ W(CO) ₃] ₂ (26t)	3.165(3)	121.9	47.0	this work
(Me ₂ C)(Me ₂ Si)[C ₅ H ₃ W(CO) ₃] ₂ (11)	3.403(2)	149.2	0	this work
(Me ₂ Si) ₂ [C ₅ H ₃ W(CO) ₃] ₂	3.260(5)	135.6(7)	28.7(4)	12
(Me ₂ Si) ₂ [C ₅ H ₃ W(CO) ₃] ₂ H ⁺	3.657(6)	149.7(2)		12

^a ∠Cp–Cp fold angle = the dihedral angle between the planes of the cyclopentadienyl ring; CEN = the centroid of the cyclopentadienyl ring.

similar structures were obtained from thermal reactions of the corresponding doubly bridged ligands with Fe(CO)₅.^{4b} The results presented here further indicated that the formation of type C complexes presents a common feature for the reactions of the carbon and silicon (or germanium) doubly bridged biscyclopentadiene ligands with metal carbonyl (M = Fe, Mo, W) compounds. Compared to the corresponding dinuclear metal complexes, the ∠Cp–Cp fold angles of the type C complexes were much smaller, suggesting that the intramolecular nonbonding interactions were highly relaxed, which is consistent with the thermal stability of these complexes.

EPR Spectra. Although the distances of the Mo–Mo bond in complexes **2** [3.4328(12) Å] and **8** [3.453(2) Å] are the longest of all the analogues known, there is no evidence for metal–metal bond homolysis in their ¹H NMR spectra. This is similar to the fulvalene complexes FvM₂(CO)₆ (M = Cr, Mo, W),^{11,14,17} another class of biscyclopentadienyl dinuclear metal complexes

Scheme 3



with long metal–metal bonds, but very different from the chromium–chromium complex [CpCr(CO)₃]₂, which shows a very broad resonance.⁹ To further study the superlong metal–metal bond, EPR experiments were performed. There was no signal in benzene solution, indicating that the long metal–metal bond is still stable in solution. Surprisingly, a distinct EPR signal (Figure 14, *g* = 2.160) was recorded for the crystal state of complex **2**, suggesting the presence of radicals in the solid state (Scheme 3). Similar observations were reported in the crystalline [CpCr(CO)₃]₂ obtained by sublimation, and the authors claimed the presence of approximately 50% of the substance as radicals according to the intense signal.¹⁸

(17) McGovern, P. A.; Vollhardt, K. P. C. *Chem. Commun.* **1996**, 1593.

(18) Keller, H. J. Z. *Naturforsch. B* **1968**, *23*, 133.

Mechanism Discussion. Our experiments on the reactions of carbon and silicon or germanium doubly bridged biscyclopentadiene ligands with different metal carbonyl compounds, namely, $\text{Fe}(\text{CO})_5$,^{4b} $\text{Mo}(\text{CO})_6$, or $\text{W}(\text{CO})_6$, gave similar and consistent results. In most cases the reactions gave a series of dinuclear metal complexes with superlong M–M bonds and the corresponding desilylation or dgermylation products, whereas the formation of the novel type C complexes depends on the ligand and metal. There is no relationship between the three types of products, meaning they cannot be converted to one another under the conditions used in the reactions. This suggests that the three types of products were formed at the same time. However, it was experimentally difficult to follow the reaction under such conditions for more detailed mechanistic studies. The exact course of the reactions still remains unclear after all the efforts. There are some reports about the cleavage of the C–Si or C–Ge bond and the migration of the silyl or germyl group.^{19–21} When $\text{C}_5\text{H}_5\text{EMe}_3$ (E = Si, Ge, Sn) reacted with $(\text{MeCN})_3\text{M}(\text{CO})_3$ (M = Cr, Mo, W), it was found that GeMe_3 and SnMe_3 could easily migrate to the metal atom to give $\text{C}_5\text{H}_5(\text{CO})_3\text{M–EMe}_3$ (M = Cr, Mo, W; E = Ge, Sn), while SiMe_3 was more difficult to transfer.^{19–21} This made us propose that the type C complexes with a W–Si or M–Ge (M = Mo, W) bond in this work could be the silyl or germyl single-migration products. For the reaction with $\text{Fe}(\text{CO})_5$ and $\text{W}(\text{CO})_6$, both ligands with carbon/silicon double bridges and carbon/germanium double bridges gave the novel type C complexes. However, for the reaction with $\text{Mo}(\text{CO})_6$, only the carbon and germanium doubly bridged ligands gave the type C complexes. Since the type C complexes contain a M–Si or M–Ge bond, their formation was apparently accompanied by the cleavage of a C–Si or C–Ge bond in the ligands. Due to the weakness of the C–Ge bond, one can predict that type C complexes with M–Ge bonds will form more readily than those with M–Si bonds. The results from our experiments

(19) (a) Heck, J.; Kriebisch, K.-A.; Mellinghoff, H. *Chem. Ber.* **1988**, *121*, 1753. (b) Xu, S.; Xie, W.; Zhou, X.; Wang, J.; Chen, H.; Guo, H.; Miao, F. *Chem. J. Chin. Univ.* **1996**, *17*, 1065.

(20) Keppie, S. A.; Lappert, M. F. *J. Organomet. Chem.* **1969**, *19*, P5.

(21) Abel, E. W.; Moorhouse S. *J. Organomet. Chem.* **1971**, *28*, 211.

were in agreement with this prediction. The bulky substituents at the bridging carbon atom (ligands **1**, **4**, **18**, and **20**) may increase the intramolecular nonbonding interactions and thus promote the silyl or germyl transfer and promote the formation of the complexes of type C (**13**, **15**, **19**, **21**, **22**, and **23**). Also supporting this is the fact that the reaction of the doubly bridged ligands with a methylene bridge (no substituent at the bridging carbon) with metal carbonyl failed to give any type C complexes. The reaction of the doubly bridged ligands with a methylene bridge with metal carbonyl cannot give the complex of type C, indicating that the repulsion between the substituents at the two bridging atoms might be the driving force of silyl or germyl transfer. On the other hand, the bulky substituents at the bridging silicon atom or on the cyclopentadienyl rings turn to prevent silyl or germyl transfer and the formation of the type C complexes.

Conclusions

Reactions of carbon and silicon or germanium doubly bridged biscyclopentadiene ligands $(\text{X})(\text{Y})(\text{C}_5\text{H}_4)_2$ with molybdenum (tungsten) carbonyl were studied. A series of doubly bridged biscyclopentadienyl dinuclear metal complexes with unusually long M–M bonds and a novel type C complexes with a M–Si or M–Ge bond were obtained. The factors affecting the structures of dimolybdenum or ditungsten complexes were discussed.

Acknowledgment. We thank the National Natural Science Foundation of China (No. 20202004), the Research Fund for the Doctoral Program of Higher Education (2000005504), and the Scientific Research Foundation for the Returned Overseas Chinese Scholars, State Education Ministry (2001-345), for financial support.

Supporting Information Available: Tables of crystallographic data collection information, final positional and thermal parameters of the non-hydrogen atoms, general temperature factors, and bond distances and angles for **2**, **6**, **8**, **10**, **11**, **13**, **14**, **15**, **19**, **21**, **22**, **25t**, and **26t**. This material is available free of charge via the Internet at <http://pubs.acs.org>.

OM034039Z